

See discussions, stats, and author profiles for this publication at: <https://www.researchgate.net/publication/51466440>

Minimally Invasive Surface-Enhanced Raman Scattering Detection with Depth Profiles Based on a Surface-Enhanced Raman Scattering-Active Acupuncture Needle

ARTICLE *in* ANALYTICAL CHEMISTRY · AUGUST 2011

Impact Factor: 5.64 · DOI: 10.1021/ac2007009 · Source: PubMed

CITATIONS

11

READS

14

5 AUTHORS, INCLUDING:



Jian Dong

Fudan University

107 PUBLICATIONS 1,450 CITATIONS

SEE PROFILE

Minimally Invasive Surface-Enhanced Raman Scattering Detection with Depth Profiles Based on a Surface-Enhanced Raman Scattering-Active Acupuncture Needle

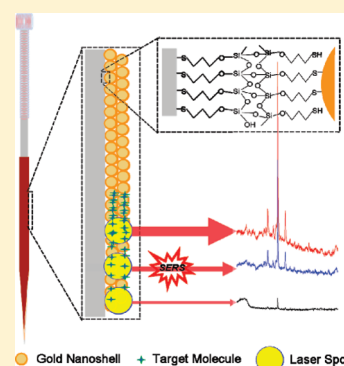
Jian Dong,^{*,†,‡} Qingfeng Chen,[†] Chunhui Rong,[†] Danyang Li,[†] and Yanying Rao[†]

[†]State Key Laboratory of Bioelectronics, Southeast University, 210096, Nanjing, China

[‡]Laboratory of Environment and Biosafety, Research Institute of Southeast University in Suzhou, 215123, Suzhou, China

 Supporting Information

ABSTRACT: To obtain depth profiles of surface-enhanced Raman scattering (SERS) information in living systems, a SERS-active needle was structured by acupuncture needles, gold nanoshells (GNSs), and polystyrene, which were used as carriers, SERS-active elements to be absorbed on the carriers, and coatings to protect the absorbed GNSs from being erased during insertion, respectively. The SERS-active needle is minimally invasive for entering and exiting the body. The interspaces between the GNSs became vessels to collect diffused fluids at different depths after a SERS-active needle was inserted into an agarose gel, and the SERS intensity profile on the SERS-active needle coincided with the concentration profile of Nile Blue A (NBA) in the gel. SERS detection in vitro avoided the signal attenuation in gels, and the SERS detection at different spots of the SERS-active needle provided a depth profile of the NBA molecule in the gel. In vivo experiments of NBA and 6-mercaptopurine confirmed that the SERS-active needle could collect fluids in living systems easily with minimal invasion and provide information about depth profiles of target molecules in tissues.



Monitoring the distribution of endogenous or exogenous molecules in target tissues rather than their concentration in blood is more important in many fields including understanding physiological mechanisms, such as neural signal transduction, assessing drug bioavailability, such as cancer chemotherapy, etc.¹ Few traditional in situ analytical methods can achieve the purpose entirely because of their invasion or extensive sample preparation. Raman spectroscopy is widely used to provide chemical and physical information based on vibrations in molecules. It is also a qualitatively or semiquantitatively analytical tool for ultrasensitive detection benefited from the design and fabrication of nanostructure with surface-enhanced Raman scattering (SERS) activity. The Raman technique is desired for monitoring biological samples in situ and real time because its application is performed without considering physical states of samples such as states, temperature, morphology, and size.²

Many attempts have been carried out to use Raman spectroscopy to detect target molecules in vivo. However, to obtain relevant SERS data in living systems is still a greater challenge. Examples include how to implant and take out the SERS materials in vivo without damage to either the host or the materials, how to avoid the immune response to the SERS materials, and with more difficulty, how to collect distinguishable SERS signal in vivo; in which case, infrared lasers used as excitation sources can transmit some biological tissues almost without attenuation, but the corresponding Raman signals transmit these tissues with difficulty. In Nie's study, the SERS

signal can be detected at 1–2 mm subcutaneously or about 10 mm in muscles.³ In Van Duyne's reports, a glass in a metal frame was placed in an incision to provide a transparent window for collecting SERS signals to avoid attenuation in the skin.⁴ Recently, a new tool that combines SERS with spatially offset Raman spectroscopy was designed to collect SERS signals in vivo directly,^{5,6} measuring the signal of implanted surface enhanced resonance Raman scattering (SERRS) nanoparticles at the maximum depth of 25 mm in muscle tissues.⁶

Acupuncture needles have been used in Chinese medicine to insert into the body for medical treatments for thousands of years. Their application has minimally invasive merits such as no bleeding and mitigation of pain.⁷ So the acupuncture needle is a promising tool for entering and exiting the body with minimal invasion. Here, the acupuncture needle was used as a carrier to absorb SERS-active nanomaterials to become a SERS-active needle. After the SERS-active needle was inserted into the body, interstitial fluids would diffuse into the interspaces between the SERS-active nanomaterials; after the SERS-active needle was pulled out, analytes in the diffused fluids at different depths were taken out. SERS detection in vitro can avoid signal attenuation in tissues, and SERS detection at different spots of the SERS-active needle can provide information about depth profiles of analytes in tissues.

Received: March 18, 2011

Accepted: July 5, 2011

Published: July 05, 2011

EXPERIMENTAL METHODS

Materials and Chemicals. The suspensions of silica colloidal particles of 55 nm in radius were obtained from Nissan Chemical Corporation (Japan). Stainless-steel acupuncture needles of 0.20 mm in diameter used in all experiments were purchased from Suzhou Tianxie Acupuncture Instruments Co. Ltd. (China). 3-Mercaptopropyltriethoxysilane was from Xiya Reagents (China). HAuCl_4 was from Guoyao Group (China). Nile Blue A (NBA) was from Sigma-Aldrich. 6-Mercaptopurine (6-MP) was from Aladdin Chemistry Co. Ltd. (China). All other reagents used were analytical grade.

Fabrication of SERS-Active Needles. To structure SERS-active materials, gold nanoshells (GNSs, consisting of a thin gold shell around a dielectric core) are one of the excellent element materials because of their perfect fabrication process, optical tunability, and larger Raman enhanced factor.^{8–11} Here, GNSs were chosen to absorb on the surface of acupuncture needles to structure a microtraumatic and SERS-active needle. The GNSs ($[r_1, r_2] = [55, 80]$ nm) were fabricated by following a reported method.⁸ The as-fabricated GNSs were centrifuged and redispersed in pure water with a concentration of 2×10^9 particles/mL. Figure 1 illustrated its structure and depth-resolution SERS detection. Stainless-steel acupuncture needles of 0.20 mm in diameter were used in all experiments. First, the needles were washed with ethanol three times; second, the needle body was immersed in 10% (v/v) of 3-Mercaptopropyltriethoxysilane ethanol solution for 48 h at 4 °C; third, the needles were washed with ethanol three times and then, the needle body was immersed in GNSs suspensions with serial concentrations (from 2×10^9 to 0.03×10^9 particles/mL diluted with a ratio of 1:4) for 24 h at 4 °C; finally, the needle body with GNSs was dipped in PS toluene solutions with serial concentrations for 3 s. After drying, the SERS-active needles were washed with 70% ethanol aqueous solution three times and then kept in sterile saline for the following experiments.

Characterizations and Measurements. SEM measurements were carried out on a Zeiss ULTRA-plus scanning electron microscope. SER spectra were obtained at room temperature (~ 20 °C) with a Renishaw Invia microRaman spectroscopy using a 785 nm excitation laser, under linefocus mode. The laser was focused onto the sample surface by using a $50\times$ long working distance objective. The extinction power was 120, 60, or $0.12 \mu\text{W}$, and the acquisition was 1 or 10 s.

Assessments of the SERS-Active Needles. NBA was used as a probe molecule in the study. The SERS-active needles with 1.25% PS coating were incubated in 1×10^{-4} M of NBA solution for 30 min to assess their reproducibility. After the needles were dried, SERS measurements were carried out with $0.12 \mu\text{W}$ laser power and 10 s acquisition time. To obtain the measurement range of NBA, the SERS-active needles were immersed in serial concentrations of NBA solutions for 30 min and then the needles at 5 mm below the liquid level were directly used for SERS measurement with $60 \mu\text{W}$ laser power and 10 s acquisition time.

To assess the feasibility of depth-resolution SERS detection of the needles, the bottom of cylindrical agarose gels (1.5% w/v) was immersed in 2×10^{-4} M of NBA solution for 4 h to form a gradient concentration contribution and then, a SERS-active needle was inserted from the top vertically. After 10 min, the needle was pulled out for SERS detection with $60 \mu\text{W}$ laser power and 10 s acquisition time. Started at 1.0 mm from the needle tip, the interval of the measured spots is 1.0 mm. Animal

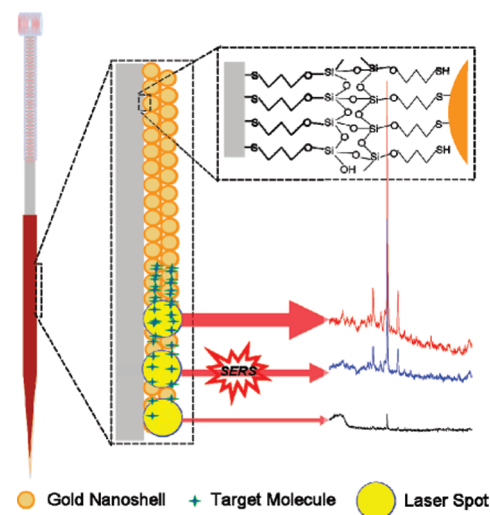


Figure 1. Illustration of the structure of a SERS-active needle and the SERS detection of a depth profile based on the SERS-active needle.

experiments were performed with the permission of the Science and Technology Department of Jiangsu Province (SYXK 2010-0004). To assess the usefulness in living systems of the SERS-active needle, a male New Zealand rabbit (about 1500 g) was anesthetized with pentobarbital at a dose of 50 mg/kg intraperitoneally. After the anesthetic had taken effect, the lateral hair of the vastus lateralis tendon was removed with scissors. NBA solution ($200 \mu\text{L}$, 2×10^{-4} M) was injected into the center of the vastus lateralis tendon, and 5 and 20 min later, two needles were inserted distally 10 mm from the previous injection spot to collect samples, respectively. The distance between the two inserted spots is about 5 mm, and the inserted depth of the needles is about 7 mm. The first needle was inserted into the tendon for 10 min, and the second was 50 min. SERS measurements were carried out immediately by using $60 \mu\text{W}$ laser power and 1 s acquisition time after the needles were pulled out. 6-MP, one of the major drugs for acute lymphoblastic leukemia, was chosen to assess the ability of SERS detection of the needles for drug molecules *in vivo*. 6-MP in 0.1 M NaOH aqueous solution (1 mL, containing 17 mg drug) was injected into the ear vein of a rabbit, and then, the SERS-active needles were inserted into the other ear vein and vastus lateralis tendon for 10 min to detect the drug concentration in blood and muscles, respectively. After the SERS-active needles were pulled out, SERS measurements were carried out immediately by using $120 \mu\text{W}$ laser power and 10 s acquisition time. Three spots at 3.0, 3.5, and 4.0 mm from the needle tip were detected, respectively. The rabbits were thermally stabilized by a homemade heating box during the experiment.

RESULTS AND DISCUSSION

The immersed depth of needles in GNSs suspensions determined the area of absorbed GNSs (Figure S-1 in the Supporting Information). The higher was the concentration of the GNSs suspension, the greater the amount of GNSs absorbed on needles (Figure S-2 in the Supporting Information) and the stronger the corresponding SERS signal. Figure 2A shows the absorbed GNSs on a needle immersed in 2×10^9 particles/mL of GNSs suspension, and GNSs almost covered the entire immersed needle body at the concentration. The absorbed GNSs would fall off during the process of inserting into the body. PS is often

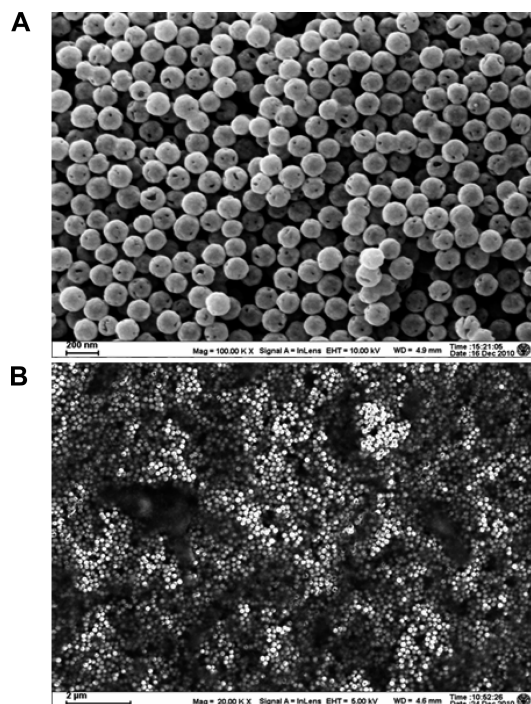


Figure 2. The SEM images of GNSs on a needle (A) and GNSs on a needle coated with 1.25% PS solution (B).

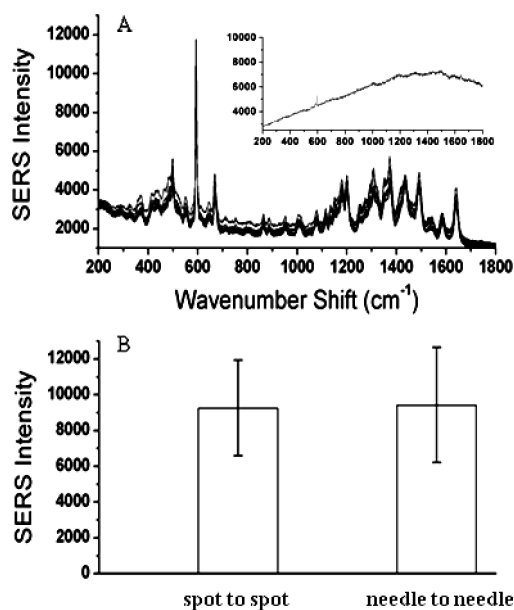


Figure 3. SERS spectra taken from eight different spots of one needle (inset is normal Raman spectrum from NBA power) (A) and the 592 cm^{-1} band intensity distribution of NBA of intraneedle and interneedles (B).

used as cell culture substrates due to its bioinertness necessary for biomedical materials used *in vivo*. Here, PS was chosen as the coating to protect the GNSs from being erased during insertion. The PS coating of low concentration cannot protect the absorbed GNSs while those of high concentration prohibit the absorption of analytes on the surface of GNSs (Figures S-3 and S-4 in the Supporting Information). Figure 2B shows a typical SEM image

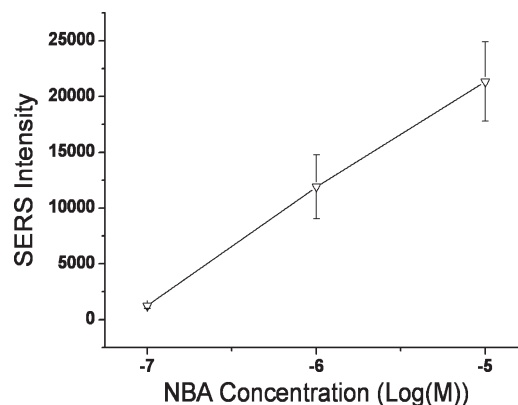


Figure 4. A plot of the 592 cm^{-1} band intensity of NBA versus concentration of NBA.

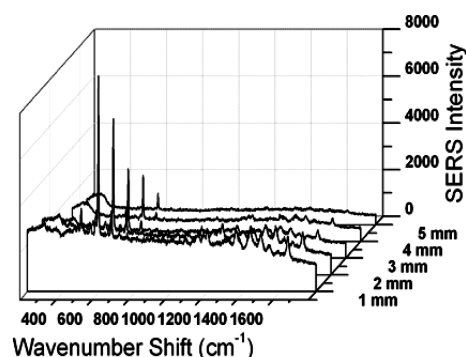


Figure 5. The NBA SERS spectra at spots with different distances from the needle tip.

of a needle with GNSs coated with 1.25% of PS toluene solution. At this concentration, the PS coating can protect the absorbed GNSs and analytes in the fluids can absorb on the surface of GNSs. The Raman signals of the SERS-active needle with PS coating are weaker than that without PS coating, perhaps because the coating occupied parts of the surface of GNSs, which decreased the absorbed amount of NBA (as shown in Figure S-4 in the Supporting Information).

The reproducibility of SERS-active needles with PS coating was assessed. As shown in Figure 3, from the SERS spectra of NBA taken from eight random spots of one needle and those taken from eight different needles, the SERS-active needles are well reproducible from spot to spot and from needle to needle. As shown in Figure 4, the needles coated with 1.25% of PS solution can be used to detect NBA aqueous solution in the range from 1×10^{-7} to 1×10^{-5} M with 60 μW laser power and 10 s acquisition time.

SERS-active needles coated with 1.25% of PS solution were used in the following experiments. Cylindrical agarose gels were used as a model of biological tissue, the bottom of a gel was immersed in NBA solution to form a concentration gradient in the gel by diffusion, and then a SERS-active needle was inserted from the top of the gel vertically. SERS measurements were carried out immediately after the needles were pulled out. As shown in Figure 5, the 592 cm^{-1} band intensity of NBA was distance-dependent. Away from the needle tip, the SERS intensity decreased gradually, which coincided with the concentration distribution of NBA in the gel. The results indicated that SERS detection based on the SERS-active needle is capable of

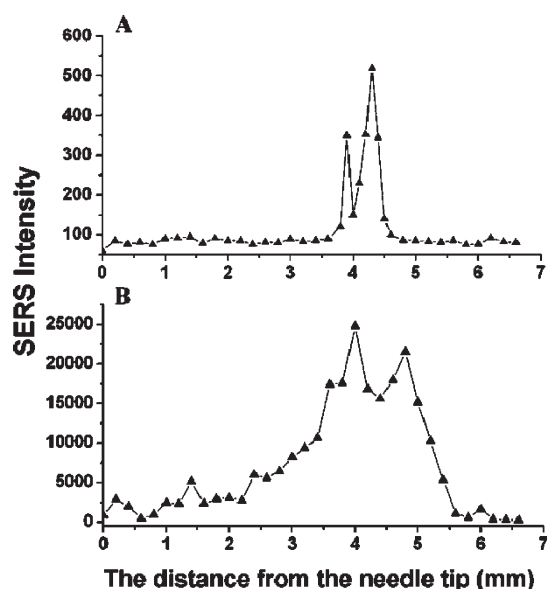


Figure 6. The 592 cm^{-1} band intensity distribution of NBA on needles pulled out after inserting for 10 (A) and 50 min (B), respectively.

monitoring the SERS-depth profile (concentration profile) of NBA in the gel. Two factors are crucial for SERS detection of depth profiles. First, after the SERS-active needle was inserted into the gel, the interspaces of the GNSs accommodated diffused samples from the corresponding depths in the gel, and after recovery was reached, the NBA concentration at different spots on the SERS-active needle was equal to that at the corresponding depths in the gel. Second, in situ detection of samples on the SERS-active needle guaranteed that the Raman intensity profile on the SERS-active needle can represent the depth profile of NBA in the gel.

Currently, the application of SERS materials to obtain information in living systems has been met with some problems. The materials should be introduced into the body by surgery for bulk materials or injection for nanoparticles, and the second surgery is necessary to take out the bulk materials while the nanoparticles almost cannot be taken out once injected. The SERS signal attenuation in tissues is also an inevitable barrier in the detection of low concentration ingredients. In contrast, it is easy and minimally invasive for the SERS-active needle entering and exiting the body; the sample at any depth where a needle can reach can be collected and its Raman signal does not decay due to the detection in vitro. Besides, SERS detection of depth profiles can provide information about the concentration profile of target molecules, while SERS detection based on the other SERS materials cannot provide similar data.

In vitro data suggested that it is feasible to collect fluids in vivo and provide depth profiles of target molecules by using the SERS-active needle. However, it should be noted that further in vivo data are essential for assessing their real usefulness in living systems.

Figure 6A shows the 592 cm^{-1} band intensity profile of NBA on a needle which was pulled out after inserting into the muscle for 10 min, and according to the SERS intensity profile, the NBA molecule only distributed on little parts of the needle. Figure 6B shows the 592 cm^{-1} band intensity profile of NBA on another needle which was pulled out after inserting for 50 min, and the molecule was almost distributed into the whole SERS-active

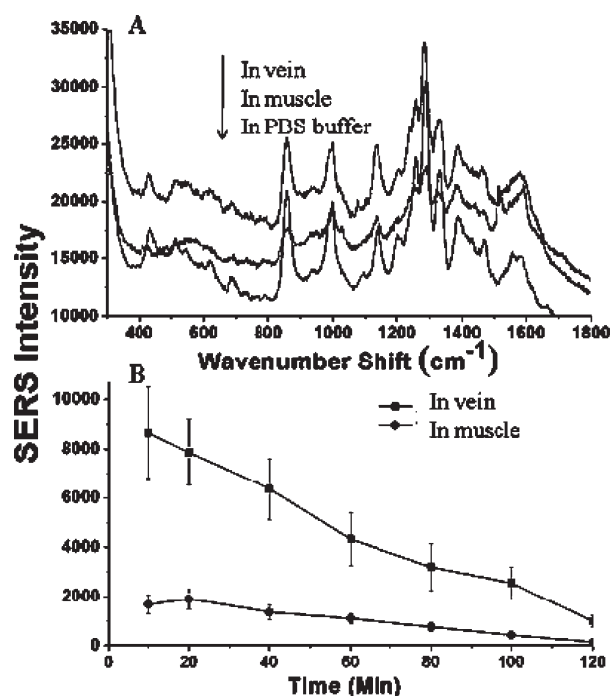


Figure 7. The SER spectra of 6-MP on the SERS-active needles inserted into the ear vein and muscles at 40 min and immersed in PBS buffer of $1 \times 10^{-3}\text{ M}$ (A) and the plots of the 858 cm^{-1} band intensity of 6-MP on needles inserted into the ear vein and muscles versus time (B).

parts of the needle. Considering the inserted depth of the needles was about 7 mm, from Figure 6A, we concluded that at this time NBA was distributed in the depths of 2.4–3.2 mm subcutaneously at the inserted spot. From Figure 6B, we concluded that at this time NBA was distributed in the whole subcutaneous space at the inserted spot, and that it was mainly concentrated in the depths of 1.5–4.5 mm subcutaneously.

6-MP has strong binding to gold substrate due to its thiol group, and its purine ring has strong SERS activity. As shown in Figure S-5 in the Supporting Information, the needles can be used to detect 6-MP in anticoagulated blood above the concentration of $1 \times 10^{-6}\text{ M}$ with $120\text{ }\mu\text{W}$ laser power and 10 s acquisition time. Figure 7A shows the spectra of 6-MP absorbed on the needles from blood, muscle, and PBS buffer, respectively. The spectra from blood and muscle are similar to that from PBS buffer, and we speculated that small biomolecules almost have no SERS signal in the spectra due to weak binding to the gold surface, weak SERS signal, or low concentration and that biomacromolecules also have no SERS signal, such as proteins absorbed on PS film that cannot pass through the PS film and absorb on the GNSs. Figure 7B shows plots of the 858 cm^{-1} band intensity of 6-MP on needles inserted in the body versus time. The concentration of free 6-MP in the body decreased after injection, and the concentration of 6-MP in blood is higher than that in muscles. The results show that the SERS-active needles can detect the free 6-MP in vivo. No existing analytical methods were adopted to verify the actual concentration profile of the two molecules in situ, but at least the present data confirmed that the SERS-active needle can collect samples easily in living systems with minimal invasion and that the SERS detection can provide depth profiles of target molecules such as NBA and 6-MP, which are Raman-active and have strong interaction with SERS materials.

To our knowledge, microdialysis is one of the available techniques that can collect extracellular tissue fluids in vivo with minimal invasion, and it has been an important tool in the research of neuroscience, pharmacology, etc.^{12–15} Recently, in vivo solid-phase microextraction (SPME) was used as a sample preparation method for global metabolomics study.¹⁶ Compared to these reports, the SERS detection based on the SERS-active needle not only has similar advantages such as sampling in vivo with minimal invasion but also has its unique advantages. More information can be obtained from one sampling: the concentration of target molecules at different depths can be provided by one sampling while the similar data can be obtained by multi-point samplings at different depths using several microdialysis probes. With a shorter time of sampling and detection, the diameter of the dialysis membrane used in CMA microdialysis is 240 μm at least and the thickness of SPME extracted coating is 45 μm , while the diffused thickness of the needle is less than 400 nm, twice the diameter of a GNS. Thus, recovery time of the needle in tissues is shorter than that of the reports. The scanning and processing time of Raman detection is also shorter than that of high-performance liquid chromatography, which is always used as an analyzer for samples of microdialysis and SPME.

CONCLUSIONS

In summary, a SERS-active needle has been fabricated by absorbing nanoscaled materials (GNSs) onto microscaled materials (acupuncture needles), which combined SERS-activity and minimal invasion. The SERS-active needle can collect samples with depth-information in vivo with minimal invasion. The SERS detection in vitro avoided signal attenuation in tissues, and the SERS detection at different spots of the SERS-active needle provided depth profiles of analytes. Generally, it is a useful strategy for enlarging SERS-detected objects by fabricating SERS materials with high enhancement factors for molecules with weak Raman-activity and functionalizing their surface to preconcentrate the target molecules with nonexistent binding to the SERS materials. With functionalization of its surface, the SERS-active needle can be used to detect various kinds of molecules of interest, which would certainly promote application of SERS in collecting information of life in situ.

ASSOCIATED CONTENT

S Supporting Information. Additional information as noted in text. This material is available free of charge via the Internet at <http://pubs.acs.org>.

AUTHOR INFORMATION

Corresponding Author

*E-mail: dongjian@seu.edu.cn.

ACKNOWLEDGMENT

We acknowledge financial support from the Natural Science Foundation of Jiangsu Province (Grant BK2010238).

REFERENCES

- (1) Chaurasia, C. S.; Muller, M.; Bashaw, E. D.; Benfeldt, E.; Bolinder, J. *Pharm. Res.* **2007**, *24* (5), 1014–1025.
- (2) Smith, E.; Dent, G. *Modern Raman Spectroscopy—A Practical Approach*; John Wiley & Sons: Hoboken, NJ, 2005; pp 135–179.

- (3) Qian, X. M.; Peng, X. H.; Ansari, D. O.; Yin-Goen, Q.; Chen, G. Z. *Nat. Biotechnol.* **2008**, *26*, 83–90.
- (4) Stuart, D. A.; Yuen, J. M.; Shah, N. C.; Lyandres, O.; Yonzon, C. R.; Glucksberg, M. R. *Anal. Chem.* **2006**, *78*, 7211–7215.
- (5) Yuen, J. M.; Shah, N. C.; Walsh, J. T.; Glucksberg, M. R.; Van Duyne, R. P. *Anal. Chem.* **2010**, *82*, 8382–8385.
- (6) Stone, N.; Faulds, K.; Graham, D.; Matousek, P. *Anal. Chem.* **2010**, *82*, 3969–3973.
- (7) Goldman, N.; Chen, M.; Fujita, T.; Xu, Q. W.; Peng, W. G. *Nat. Neurosci.* **2010**, *13*, 883–888.
- (8) Oldenburg, S. J.; Averitt, R. D.; Westcott, S. L.; Halas, N. J. *Chem. Phys. Lett.* **1998**, *288*, 243–247.
- (9) Jackson, J. B.; Westcott, S. L.; Hirsch, L. R.; West, J. L.; Halas, N. J. *Appl. Phys. Lett.* **2003**, *82*, 257–259.
- (10) Talley, C. E.; Jackson, J. B.; Oubre, C.; Grady, N. K.; Hollars, C. W. *Nano Lett.* **2005**, *5*, 1569–1574.
- (11) Wang, H.; Kundu, J.; Halas, N. J. *Angew. Chem., Int. Ed.* **2007**, *46*, 9040–9044.
- (12) Hernandez, G.; Haines, E.; Shizgal, P. J. *Neurosci. Methods* **2008**, *175*, 79–87.
- (13) Mou, X.; Lennartz, M. R.; Loegering, D. J.; Stenken, J. A. *Biomaterials* **2010**, *31*, 4530–4539.
- (14) Ungerstedt, J.; Nowak, G.; Ungerstedt, U.; Ericzon, B. G. *Liver Transplant* **2009**, *15*, 280–286.
- (15) Blakeley, J. O.; Olson, J.; Grossman, S. A.; He, X. Y.; Weingart, J.; Supko, J. G. *J. Neuro-Oncol.* **2009**, *91*, 51–58.
- (16) Vuckovic, D.; de Lannoy, I.; Gien, B.; Shirey, R. E.; Sidisky, L. M.; Dutta, S.; Pawliszyn, J. *Angew. Chem., Int. Ed.* **2011**, *50*, 5344–5348.